Supporting information for:

Single-Molecule Tip-Enhanced Raman Spectroscopy of C_{60} on the Si(111)-(7×7) Surface

Borja Cirera[a,b*], Shuyi Liu[a,c], Youngwook Park[a], Ikutaro Hamada[d], Martin Wolf[a], Akitoshi Shiotari[a] and Takashi Kumagai[a,e]

[a.] *Department of Physical Chemistry, Fritz-Haber Institute of the Max-Planck Society, Faradayweg 4-6, 14195 Berlin, Germany*

[b.] *Instituto de Ciencia de Materiales de Madrid (CSIC). c/ Sor Juana Inés de la Cruz 3. Campus de Excelencia de la Universidad Autónoma de Madrid. 28049, Spain*

[c.] *Wuhan National Laboratory for Optoelectronics, Huazhong University of Science and Technology, Wuhan, China*

[d.] *Department of Precision Engineering, Graduate School of Engineering, Osaka University, 2-1 Yamadaoka, Suita, Osaka 565-0871, Japan*

[e.] *Center for Mesoscopic Sciences, Institute for Molecular Science, Okazaki 444-8585, Japan*

corresponding author: borja.cirera@csic.es

Table of content:

1. Methods for sample preparation and SPM-TERS measurements

Sample preparation. All experiments were performed in ultra-high vacuum (UHV) chambers (base pressure $< 5 \times 10^{-10}$ mbar). We used an n-type Si(111) wafer (resistance: 0.03–0.08 Ω, thickness: 0.5 mm). The sample was degassed at ~800 K in the chamber overnight, then it was annealed several times by direct current heating to ~1470 K for 10 seconds. The C_{60} molecule was purchased from Aldrich and used without further purification. The molecules were evaporated at 610 K from a K-cell evaporator onto the substrate held at room temperature.

STM measurement. We used a low-temperature STM from UNISOKU Co., Ltd. (modified USM-1400) operated with Nanonis SPM Controller (SPECS GmbH). The bias voltage (V_{bias}) was applied to the sample, and the tip was grounded. The tunnelling current (j_{STM}) was collected from the tip. We used Ag tips fabricated by focused ion beam milling[S1]. Temperature of the system (80 or 10 K) is indicated in each figure caption.

TERS measurement. The excitation laser was focused to the STM junction with an in-situ Ag-coated parabolic mirror (numerical aperture of ~0.6) mounted on the cold STM stage. The parabolic mirror was precisely aligned using piezo motors (Attocube GmbH), which allow three translational and two rotational motions. For the Raman measurements we used a HeNe laser for 633 nm (Laser 2000 GmbH) and a solid-state laser for 532 nm (Cobolt). The incident beam is linearly polarized along the tip axis (p-polarization). The scattered photons are collected by the same parabolic mirror and detected outside of the UHV chamber with a grating spectrometer (AndorShamrock 303i). Regarding the data processing, the Raman spectra shown in Figure 2 of the main text and **Figure S2** are baseline-corrected by using the asymmetrically reweighted penalized least squares (arPLS) method[S2].

2. Raman maps

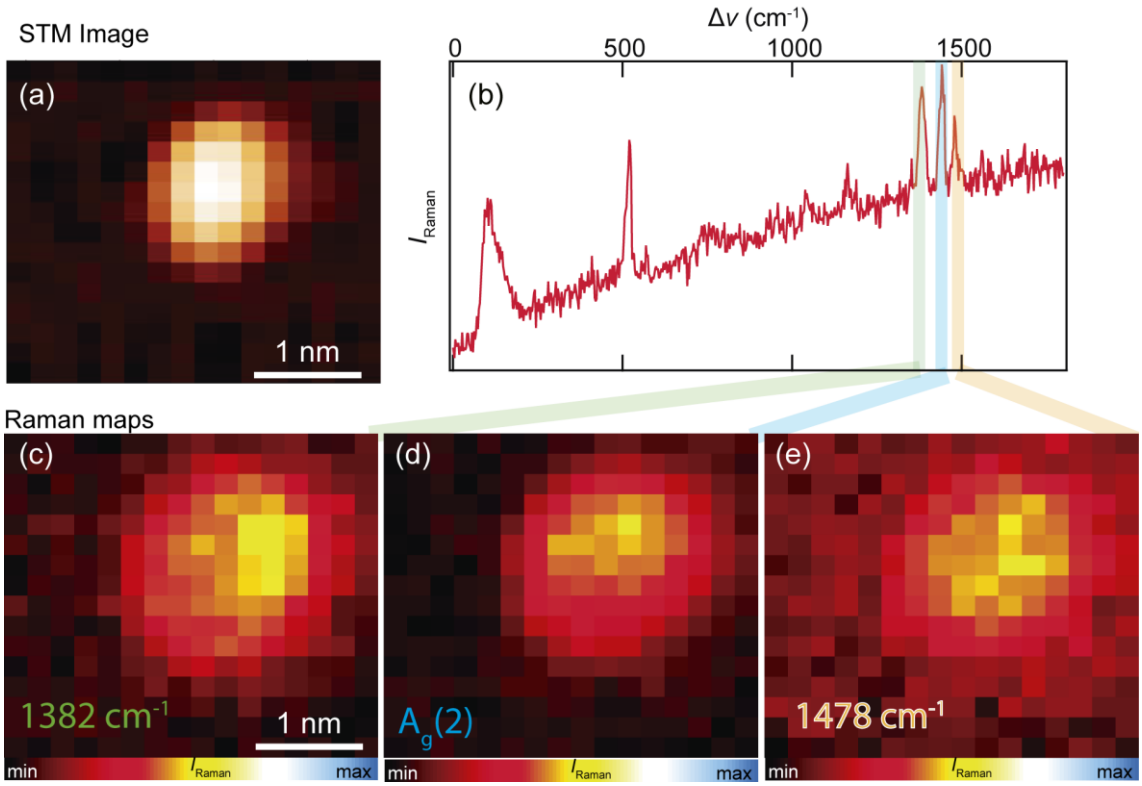

Figure S1. (a) STM image under illumination for single C_{60} on the faulted half unit cell of the Si(111)-7x7 surface (80 K, V_{bias} = 0.3 V, j_{STM} = 60 pA). **(b)** TERS spectrum of the C_{60} in (a) where the three high frequency vibrational modes at 1382, 1441 and 1478 cm^{-1} are observed (80 K, V_{bias} = 0.3 V, j_{STM} = 50 pA, λ_{ext} = 532 nm, P_{ext} = 5.5 mW). **(c-e)** TERS maps of the different peaks marked in (b). Each of the scale bars is independent and in arbitrary units for clarity.

3. Estimation of the enhancement factors

To estimate the enhancement factor of a single C_{60} TERS on the Si(111)-(7x7) surface, we compare the TERS intensity of the $A_g(2)$ mode to the Raman peak of the optical phonon mode of the bulk Si. Since the phonon peak remains constant regardless of the tip position[S3], it can be used as a reference of the Raman scattering intensity. The total effective enhancement factor g_{total} is given by:

$$g_{\mathrm{total}} = \frac{\Gamma_{\mathrm{NF}}}{\Gamma_{\mathrm{FF}}} \cdot \frac{N_{\mathrm{Si}}\sigma_{\mathrm{Si}}}{N_{\mathrm{C_{60}}}\sigma_{\mathrm{C_{60}}}}, \quad (1)$$

where $\Gamma_{\mathrm{FF\ (NF)}}$ is the far-(near-) field Raman scattering rate, N_{Si} is the number of the Si atoms within the illuminated volume, and $N_{\mathrm{C_{60}}} = 1$ is the number of C_{60}, and $\sigma_{\mathrm{Si\ (C_{60})}}$ is the Raman cross section of Si (C_{60}). As evident in Figures 1 and 2 of the main text, the Raman intensities of far-field bulk Si phonon peak and near-field C_{60} $A_g(2)$ peak are comparable; $\Gamma_{\mathrm{FF}} \approx \Gamma_{\mathrm{NF}}$.

Therefore, Equation (1) is rewritten as follows:

$$g_{\mathrm{total}} \approx \frac{\sigma_{\mathrm{Si}}}{\sigma_{\mathrm{C_{60}}}} \cdot \rho_{\mathrm{Si}} \cdot 2\pi \left(\frac{d_{\mathrm{laser}}}{2}\right)^2 d_{\mathrm{p}}, \quad (2)$$

where $\rho_{\mathrm{Si}} = 4.992 \times 10^{22}\ \mathrm{atoms\ cm^{-3}}$ is the Si atom density[S4], $d_{\mathrm{laser}} = 3\ \mu\mathrm{m}$ is the diameter of the Gaussian-beam spot[S1], $d_{\mathrm{p}} = 1.3 \times 10^{-4}\ \mathrm{cm}$ is the penetration depth in Si at 530 nm (Ref. **S5**).

References **S4** and **S6** show the cross section of Si at 785 nm is $(1.0 \pm 0.2) \times 10^{-27}\ \mathrm{cm^2}$ and the differential cross section of C_{60} at 752 nm is $(2.1 \pm 0.3) \times 10^{-29}\ \mathrm{cm^2/sr}$, respectively. According to the Rayleigh scattering formula, the cross section is proportional to the minus fourth power of the wavelength. We derive $\sigma_{\mathrm{Si}} = 4.7 \times 10^{-27}\ \mathrm{cm^2}$ and $\sigma_{\mathrm{C_{60}}} = 1.0 \times 10^{-27}\ \mathrm{cm^2}$ at 532 nm. From Equation (2), thus, we get:

$$g_{\mathrm{total}} \approx 10^{12}.$$

The total enhancement factor g_{total} is the product of the chemical enhancement factor g_{Chem} and the electromagnetic enhancement factor g_{EM}:

$$g_{\mathrm{total}} = g_{\mathrm{chem}} \cdot g_{\mathrm{EM}}. \quad (3)$$

Taking $g_{EM} \propto \left(\frac{|E_Z|}{|E_0|}\right)^4 \approx 10^9$ from Reference **S7**, where the EM field in an Ag-tip–Si-surface junction in the tunnelling regime was simulated, we obtain $g_{\mathrm{chem}} \approx 10^3$.

4. TERS spectra in the tunnelling regime with the Si signal subtracted

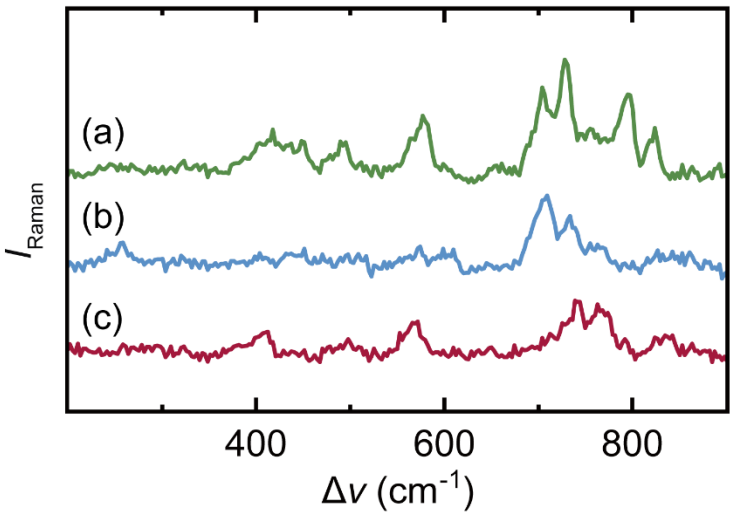

Figure S2. Si-bulk-phonon-peak-subtracted version of Figures 2a–c in the main text for better visualization of low frequency region. The intensity of each spectrum was normalized based on the bulk phonon peak intensity (Figure 2d) before subtraction.

5. Comparison of the observed C_{60} vibrational frequencies

Table S1. TERS observed peak frequencies (in cm^{-1}) for single C_{60} molecules on Si(111) of the present experiment (blue columns) and previous experiments (grey columns)

TERS, single C_{60} on Si(111) [a]					
Mol #1 (Fig. 2a)	**Mol #2** (Fig. 2b)	**Mol #3** (Fig. 2c)	**TERS, island on Ag(111)** [a,b]	**Raman, solid** [a,c]	**Assignment**
247 w	256 w		274 s	273 m	H_g**(1)**
418 w		410 vw			
448 w	443 vw		423 w	437 w	H_g**(2)**
492 sh		487 sh	492 s	496 m	A_g**(1)**
577 m		569 w			
704 m	707 m		712 w	710 w	H_g**(3)**
728 m	734 sh	742 w			
797 m	760 sh	766 w	768 m	774 w	H_g**(4)**
821 w		835 vw			
921 w	927 w	934 vw			
1054 w	1054 w	1041 m			
1028 w					
	1082 w		1099 vw	1103 w	H_g**(5)**
1156 w	1131 w	1164 m 1187 w			
1225 w			1250 vw	1256 w	H_g**(6)**
	1402 s				
1416 m	1419 sh 1432 sh		1428 sh	1435 w	H_g**(7)**
		1377 s			
1446 s	1446 s	1441 s	1470 s	1466 s	A_g**(2)**
	1481 w	1483 m			
	1503 m				
1564 s	1564 s 1583 sh	1559 w	1575 w	1576 m	H_g**(8)**

[a] vw: very weak, w: weak, m: medium, s: strong, sh: shoulder.

[b] Ref. S8.

[c] Ref. S9.

[d] R: Raman active, IR: infrared active.

[e] Ref. S10.

6. Detection of adsorption-site switching of a C_{60} molecule

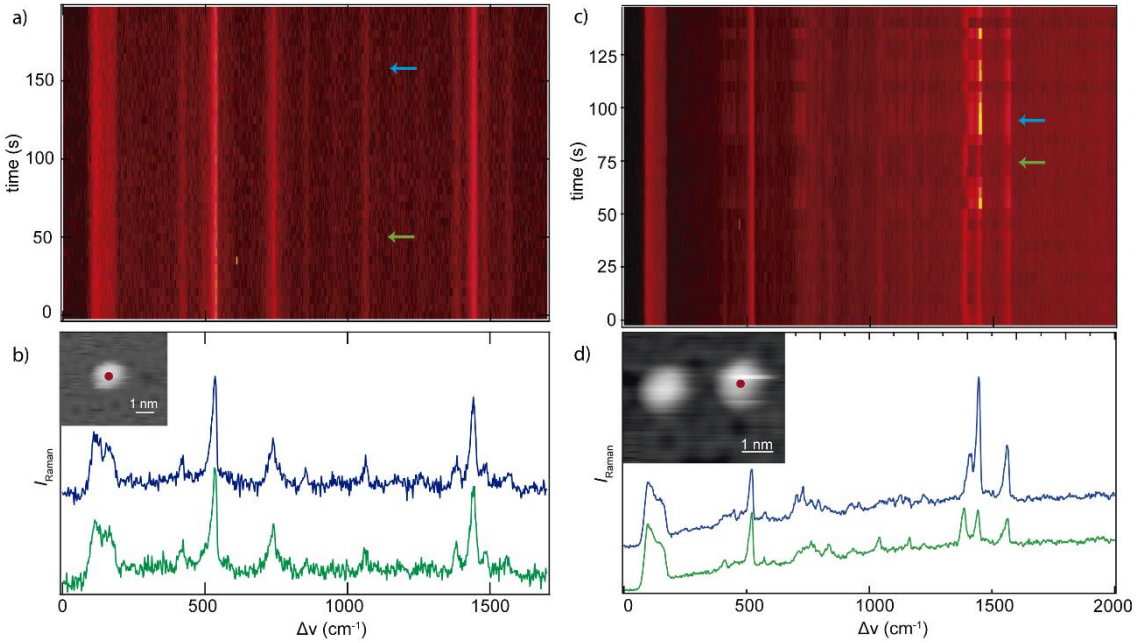

Figure S3. (a) Waterfall plot of the time evolution of the TERS signal in the tunnelling regime of a single C_{60} molecule adsorbed on the fault half unit cell (red dot, see inset below), stable over time at large tunnelling currents (5 s per spectrum, 10 K, V_{bias} = 0.3 V, j_{STM} = 5 nA, λ_{ext} = 532 nm, P_{ext} = 5.5 mW). **(b)** The two TERS spectra (blue and green arrows in a) showing stability over time. **(c)** Same as in a for another C_{60} molecule, but in this case the time evolution clearly shows the transition between two bistable states (5 s per spectrum, 10 K, V_{bias} = 0.3 V, j_{STM} = 100 pA, λ_{ext} = 532 nm, P_{ext} = 5.5 mW). **(d)** STM image of two single C_{60} molecules adsorbed on the fault half unit cell, with the right one showing brighter strips corresponding to subtle displacements originated with the tip scanning motion. The two TERS spectra (blue and green arrows in c) correspond to each of the bistable states observed in the waterfall plot.

7. Observation of the overtones and combination bands in the MPC regime in the faulted and unfaulted half unit cells

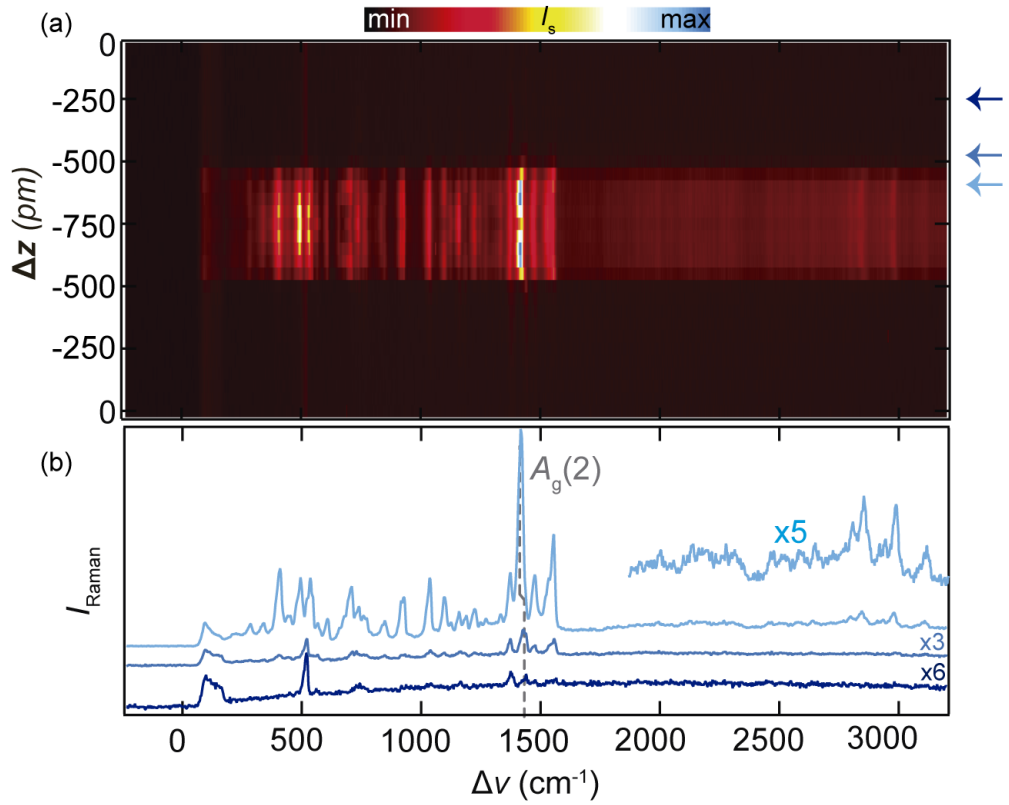

Figure S4. (a) Waterfall plot of TERS as a function of the tip height recorded during tip-approach and retraction over single C_{60} on the faulted half unit with the overtones and combination bands at higher frequencies (80 K, V_{bias} = 0.3 V, j_{STM} = 60 pA, λ_{ext} = 532 nm, P_{ext} = 5.5 mW, 5s/spectrum, Scale bar: arbitrary units). **(b)** TERS spectra in the tunnelling and contact regimes acquired at the positions of the corresponding arrow in a, highlighting that the overtones are only observed in the contact regime.

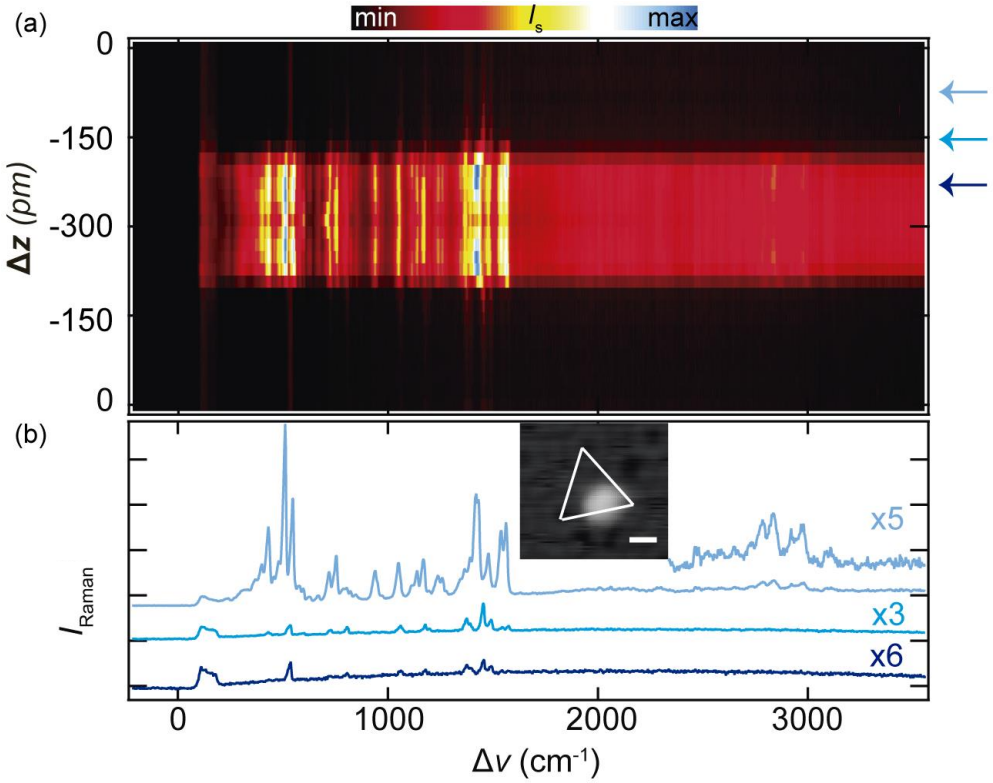

Figure S5. (a) Waterfall plot of TERS as a function of the tip height recorded during tip-approach and retraction over single C_{60} on the unfaulted half unit with the overtones and combination bands at higher frequencies (80 K, V_{bias} = 0.3 V, j_{STM} = 10 pA, λ_{ext} = 532 nm, P_{ext} = 5.5 mW, 5s/spectrum, Scale bar: arbitrary units). **(b)** TERS spectra in the tunnelling and contact regimes acquired at the positions of the corresponding arrow in a, highlighting that the overtones are only observed in the contact regime.

References

S1 S. Liu, M. Müller, Y. Sun, I. Hamada, A. Hammud, M. Wolf, and T. Kumagai, "*Resolving the correlation between tip enhanced resonance Raman scattering and local electronic states with 1 nm resolution*", *Nano Lett.*, **2019**, 19, 8, 5725-5731.

S2 S.-J. Baek, A. Park, Y.-J. Ahn, and J. Choo, "*Baseline correction using asymmetrically reweighted penalized least squares smoothing*", *Analyst*, **2015**, *140*, 250.

S3 S. Liu, A. Hammud, M. Wolf and T. Kumagai, "*Atomic Point Contact Raman Spectroscopy of a Si(111)-(7x7) Surface"*, *Nano Lett.* **2021** 21, 9, 4057-4061

S4 R.L. Aggarwal, L.W. Farrar, S.K. Saikin, A. Aspuru-Guzik, M. Stopa, D.L. Polla, "*Measurement of the absolute Raman cross section of the optical phonon in silicon*", *Solid State Commun.* **2011** 151, 553.

S5 M. A. Green, "Self-consistent optical parameters of intrinsic silicon at 300 K including temperature coefficients", Sol. Energy Mater. Sol. Cells **2008** 92, 1305–1310.

S6 J.D. Lorentzen, S. Guha, J. Menéndez, P. Giannozzi, S. Baroni," *Raman cross section for the pentagonal-pinch mode in buckminsterfullerene C_{60}*", *Chem. Phys. Lett.* **1997**, 270, 129-134.

S7 R.-P. Wang, C.-R. Hu, Y. Han, B. Yang, G. Chen, Y. Zhang, Y. Zhang and Z.-C. Dong, "*Sub-Nanometer Resolved Tip-Enhanced Raman Spectroscopy of a Single Molecule on the Si(111) Substrate*", *J. Phys. Chem. C*, **2022**, *126*, 12121–12128

S8 B. Cirera, Y. Litman, C. Lin, A. Akkoush, A. Hammud, M. Wolf, M. Rossi, T. Kumagai, "*Charge transfer-mediated dramatic enhancement of Raman scattering upon molecular point contact formation*", *Nano Lett.* **2022**, *22*, 6, 2170-2176.

S9 D. S. Bethune, G. Meijer, W. C. Tang, H. J. Rosen, W. G. Golden, H. Seki, C. A. Brown, M. S. de Vries, "*Vibrational Raman and infrared spectra of chromatographically separated C_{60} and C_{70} fullerene clusters*", *Chem. Phys. Lett.* **1991**, *179*, 181–186.

S10 J. Menéndez and J.B. Page, "*Vibrational Spectroscopy of C_{60}*", in "Light Scattering in Solids VIII," ed. by M. Cardona and G. Güntherodt, Springer, Berlin, 2000.